Investigation of gap resonance in moonpools at forward speed using a non-linear domain-decomposition method

Arnt G. Fredriksen[1], Trygve Kristiansen[1] and Odd M. Faltinsen[1]
[1]Department of Marine Technology,
Centre for Ships and Ocean Structures,
Norwegian University of Science and Technology, Trondheim, Norway
Corresponding author: arnt.g.fredriksen@ntnu.no

Introduction. Gap resonance problems have over the years been studied with either incoming waves only or forced oscilllations only. But in industrial applications ship operations involving use of moonpools is often performed in low forward speed or under the influence of a strong current. This work aims at being a step on the way to understand the effect of wave-current interaction on the water motion inside a moonpool.

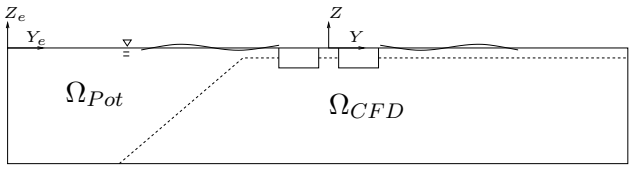

Figure 1: Overview of numerical setup. The viscous domain stretches all the way downstream, apart from the top layer that is solved by potential flow assumptions. Depth of the tank is 1.0m, draft D = 0.18m, gap width b = 0.18m, breadth of one side hull B = 0.36m.

Numerical method. Since this work is inspired by (Kristiansen and Faltinsen 2011) we started out with the aim of keeping their low computational time. To achieve this, the matrix system must be inverted once at the beginning of the simulation, and multiplied with the right hand side (RHS) each timestep. To be able to capture the wave-current interaction, it is not sufficient with a linear free-surface condition. By using a perturbation method up to second order in ζ on the free surface condition around z=0, we hoped to maintain this simple structure. Since we wanted a strong coupling between the viscous and potential domain, we needed to solve for a total velocity potential ϕ, or the acceleration potential ψ as in (Kristiansen and Faltinsen 2011), and not for two pertubation potentials, ϕ_1 for the 1st order terms and ϕ_2 for the 2nd order terms as in a standard Stokes expansion. By doing this we got one value of ϕ for each cell as in the linear problem, and this could be matched to the viscous domain at the intersection. However, spurious non-physical higher harmonics evolved in the solution. Perhaps some kind of filtering technique can be applied to remove these non-physical higher harmonics.

In the following text we give the basic outline of our numerical method. For the piston mode problem in forced heave oscillation at forward speed, we need to consider two main physical effects: the vortex seperation from the hull edges and wave generation and propagation. Therefore we propose a scheme with a fully non-linear free surface condition in the potential flow domain, coupled with a Navier Stokes flow solver for the viscous domain. Another feature is that we solve the equations in an accelerated coordinate system following the body. The advantage is that the body boundary condition is satisfied on its exact po-

sition. However the bottom boundary condition changes and is no longer exact, so instead a linear condition is applied at the mean position of the bottom boundary. An advantage of using body-fixed coordinate system is that we avoid the problem of accelerating the water in the whole tank up to a steady current.

The following governing equation is valid for the irrotational flow of an incompressible and inviscid fluid,

$$\nabla^2\phi = 0 \quad \text{in } \Omega_{Pot} \tag{1}$$

where ϕ is the absolute velocity potential defined as $\mathbf{u} = \nabla\phi$, i.e. the fluid velocity seen in an Earth-fixed coordinate system. We solve for the non-linear free-surface problem for ϕ since it satisfies Laplace's equation, which is not the case for the non-linear acceleration potential ψ. The governing equations for mass and momentum conservation in an incompressible, viscous fluid in a body-fixed coordinate system are, when only sway and heave are considered,

$$\nabla \cdot \mathbf{u}_r = 0 \quad \text{in } \Omega_{CFD} \tag{2}$$

$$\frac{\partial \mathbf{u}_r}{\partial t} + \mathbf{u}_r \cdot \nabla \mathbf{u}_r = -\frac{1}{\rho}\nabla p + \mathbf{g} + \nu\nabla^2\mathbf{u}_r - \mathbf{a}_0 \quad \text{in } \Omega_{CFD} \tag{3}$$

where $\mathbf{u}_r$ is the fluid velocity relative to the body-fixed coordinate system. The extra term $\mathbf{a}_0$ is the sway and heave acceleration of the body fixed coordinate system. The method could be generalized to include angular motions. Terms like the Coriolis acceleration would then appear on the RHS of equation (3). See (Faltinsen and Timokha 2009) for more details on the relations between a inertial and a noninertial coordinate system. The projection method by (Chorin 1968) is used to step the solution in time in the viscous domain.

Both equations (1) and (3) are solved by using the Finite Volume Method (FVM) on a staggered grid, where the pressure $\tilde{p} = p/\rho + gz$ or ϕ nodes are located in the middle of each cell, and the velocity nodes are located at the middle of the cell edges.

On the intersection line between the viscous and potential domain we require that the pressure and the normal velocity are continuous. The pressure in the potential region is found from the Bernoulli equation in a noninertial coordinate system:

$$-\frac{p}{\rho} - \frac{\partial\phi}{\partial t} - \frac{1}{2}|\nabla\phi|^2 + \mathbf{u}_0 \cdot \nabla\phi - gz = 0 \quad \text{in } \Omega_{Pot} \tag{4}$$

where $\mathbf{u}_0$ is the forced sway and heave velocity. The pressure $\tilde{p}$ in the viscous region is found when solving a Poisson equation in the projection method,

$$\nabla^2\tilde{p} = \frac{\nabla \cdot \mathbf{u}_r^{**}}{\Delta t} \quad \text{in } \Omega_{CFD} \tag{5}$$

where $\mathbf{u}_r^{**}$ is a tentative velocity field after the advection and diffusion steps are applied. The method for advection is a simple linear upwind scheme. This may argued to be good enough for the zero Froude number case, where the shed vorticity is important for about half a period. However for the non-zero Froude number cases, the shed vorticity and wake from the leading edge interact with the shed vorticity from the edges of the moonpool, and is perhaps inaccurate. On the intersection we require that the normal velocity should be continuous, i.e. seen from the potential side $\mathbf{u}_r^{n+1} = \nabla\phi - \mathbf{u}_0$ should be equal to the velocity update at next timestep seen from the viscous side, $\mathbf{u}_r^{n+1} = \mathbf{u}_r^{**} - \Delta t\nabla\tilde{p}$. Then we can setup an expression for $\mathbf{u}_r^{**}$ in the intersection region and guarantee continuity in the normal velocity. Finally we obtain one matrix system where both the potential and viscous domain are included, with the absolute velocity potential ϕ as an unknown in the potential domain, and the pressure $\tilde{p}$ as an unknown in the viscous domain.

Free-surface boundary conditions. We have applied a fully nonlinear free-surface condition. We track the free surface ζ in time and satisfy the FS condition on the exact free surface. To get accurate derivatives close to $z = \zeta$ a regridding scheme of the top layer of the potential domain is implemented, this is done every time-step. This includes the free-surface nodes and the top Nr nodes in the vertical direction, where Nr is

an input parameter to the simulation. Regridding is only applied in the potential domain, which means that for higher forcing amplitudes the viscous domain in the gap is decreased. The semi-Lagrangian kinematic and dynamic free-surface conditions in a body-fixed coordinate system then look like:

$$\frac{\partial \zeta}{\partial t} = \frac{\partial \phi}{\partial z} - \frac{\partial \phi}{\partial y}\frac{\partial \zeta}{\partial y} + \dot{\eta}_2 \frac{\partial \zeta}{\partial y} - \dot{\eta}_3 \quad \text{at } z = \zeta \quad (6)$$

$$\frac{d\phi}{dt} = -g\zeta - \frac{1}{2}\left(\frac{\partial \phi}{\partial y}\right)^2 + \frac{1}{2}\left(\frac{\partial \phi}{\partial z}\right)^2 + \dot{\eta}_2\left(\frac{\partial \phi}{\partial y} + \frac{\partial \zeta}{\partial y}\frac{\partial \phi}{\partial z}\right) - \frac{\partial \phi}{\partial z}\frac{\partial \phi}{\partial y}\frac{\partial \zeta}{\partial y} \quad \text{at } z = \zeta \quad (7)$$

Here $\dot{\eta}_2$ and $\dot{\eta}_3$ are the forced sway and heave velocity, and $d\phi/dt$ expresses the time rate of change of ϕ on the free surface, as one travels with the wave vertically.

As we regrid close to the free surface the line between the cell nodes are no longer orthogonal to the cell edge. I.e. simple finite difference between the nodes does no longer give the flux in the correct direction. We therefore construct a plane defined by the 3 nearest points, and take the derivative of this plane in the direction normal to the cell edge. By doing this the matrix system change every time-step and the low computation time by (Kristiansen and Faltinsen 2011) is lost.

The solution of equations (6) and (7) are evolved in time by an explicit fourth order Runge-Kutta method. The matrix system is solved four times each timestep by the biconjugate gradient stabilized method (BiCGSTAB).

Experimental method and setup. In this paper we will focus on the variation of the current/-forward speed, from Fn = 0 to Fn = 0.08. Here the Froude number is defined based on the total length of the two hulls including the gap (which for our case is 0.90m), i.e. Fn $= U/\sqrt{g(2B+b)}$. The tank length (5.6m of rails) limited us from testing for currents above Fn = 0.1. Even for this current it can be argued that some of the time-series have not reached steady state. The results presented here will be for 3 different Froude numbers (0.0, 0.04 and 0.08).

Forced harmonic heave motion with no incident waves was studied. Every test have been repeated twice. The model was towed in one direction, then waited 200s for the waves and wake generated by the model to die out, then towed back in the opposite direction. The cycle start again after a new 200s break with a different frequency/amplitude/-carriage velocity.

Results. Numerical setup: Both hulls and the gap share the same $\Delta y = 0.01$m. In the upstream direction, Δy is smoothly ramped up to $\lambda/30$ over 0.3m. λ is the wave length without any current present. Then Δy constant equal to $\lambda/30$ until the damping zone is reached 4λ away from the ship. Then it is smoothly ramped up to $\lambda/10$, and remains this value the rest of the 4λ long damping zone. On the downstream side Δy is smoothly ramped up to $\lambda/30$ over 0.54m. Then it is constant equal to $\lambda/30$, and then the damping zone is symmetric to the upstream side. The numerical timestep was either limited by the CFL-number=0.5 or by 120 timesteps for each period of oscillation. For the discretization in z-direction, a fixed number of 25 cells over the body has been used in all simulations. Below that, the grid size is smoothly increased such that there is a total of 55 cells in the z-direction over the total depth.

As a first observation from figure (2), the current has no significant influence on the piston mode resonance in the Froude number range tested in this work. There is a small decrease in the piston mode amplitude with 5mm and 10mm heave amplitude from Fn = 0.04 to Fn = 0.08. A probable reason might be that the leading edge create a wake that give a local velocity close to the moonpool equal to the zero Froude number case. However in the numerics we tried starting the viscous domain downstream of the first leading edge, i.e. potential non separating flow around this edge. This gave similar numerical results, indicating that the wake from the first edge is of

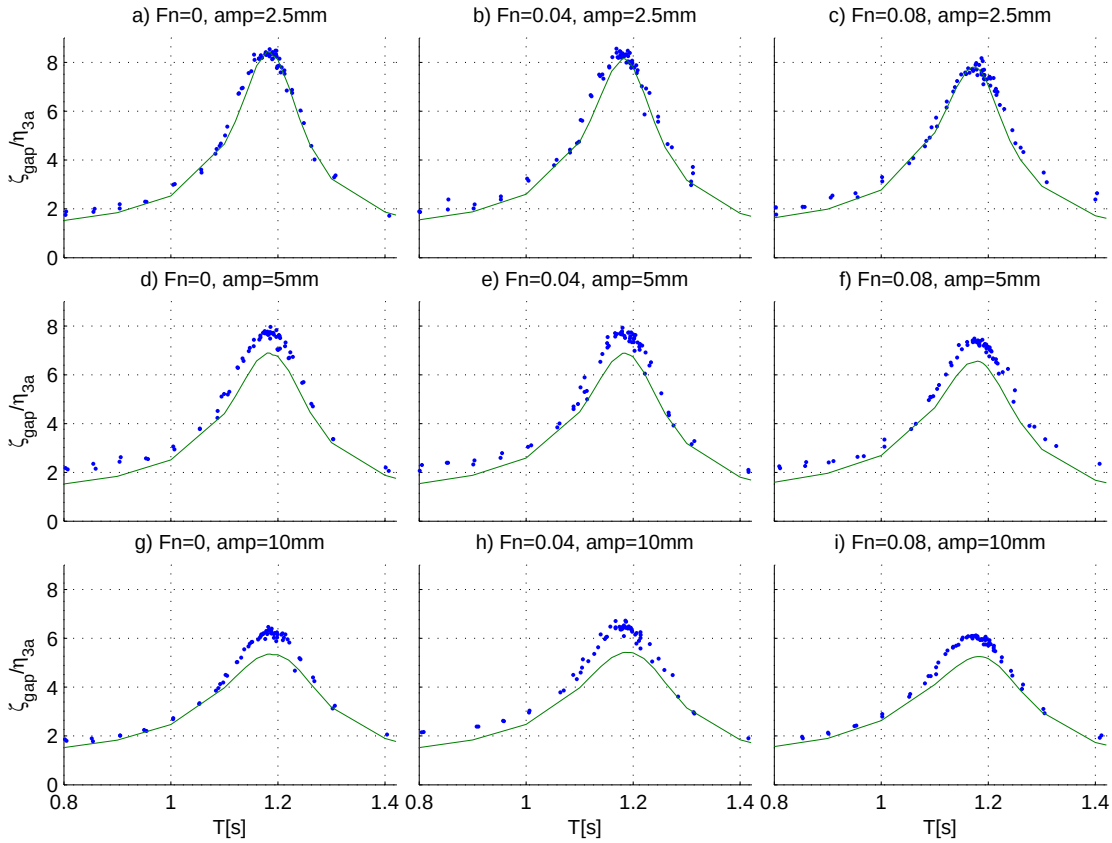

Figure 2: Comparison between experiments in blue circles against numerical results in green line. For 3 different heave amplitudes and 3 different Froude numbers.

secondary importance.

For higher heave amplitudes we see larger discrepancies between the numerics and the experiments. A reasons for the difference is that the vorticity inside the gap reaches the intersection between the potential and viscous domain. We will also perform an error analysis of the experiments.

Ongoing and future work. We are presently continuing the parameter study by including effects of draft, gap width and edge profile. Another issue we want to study is the energy transfer between the piston mode and the sloshing modes. This becomes important for increasing gap widths, when at the same time the damping from the vortex generation at the edges becomes less important.

References

Chorin, A. J. (1968). Numerical solution of the Navier-Stokes equations. *Mathematics of Computation 22*, 742–762.

Faltinsen, O. M. and A. N. Timokha (2009). *Sloshing*. Cambridge.

Kristiansen, T. and O. M. Faltinsen (2011). Gap resonances analyzed by a domain-decomposition method. In *26th Int. Workshop on Water Waves and Floating Bodies*.